PHYSICAL REVIEW B VOLUME 47, NUMBER 4 15 JANUARY 1993-II

Structural properties and energetics of amorphous forms of carbon

P. C. Kelires
Physics Department, University of Crete and Research Center of Crete, 71110 Heraklion, Crete, Greece
(Received 16 June 1992)

We have made a comparative theoretical study of the most common forms of unhydrogenated amorphous carbon (α-C), namely, of the dense, diamondlike phase and the low-density evaporated α-C (e-C). Emphasis is given to the connection among the structure, energetics, and stability of these phases. To make the simulations of the amorphous structures (formed by quenching the liquid) tractable, we used the Monte Carlo method, combined with the empirical-potential approach. Our analysis employs a powerful total-energy-partitioning scheme, which is proved very useful in treating the energetics of disordered systems. It is found that threefold sp^2 sites are the energetically favorable geometries in e-C, and thus they are by far more numerous. The nonplanar character of sp^2 sites and the absence of sixfold rings indicate that medium-range order is rather not significant in e-C. The increasing graphitic character of e-C, as the temperature is raised, is explained by resorting to the effective temperatures T^*, at which the atoms freeze in their lattice positions. For diamondlike α-C, the simulations show that there exist two distinctly different dense structures. The "as-quenched" one (i-C) is mostly sp^3 bonded, but it is metastable. Upon annealing, it converts into a second phase (i-C*), mostly sp^2 bonded, with a significant energy gain. A specific mechanism is proposed for this transition. The insensitivity of density to annealing is explained if we use the concept of the "glass transition temperature" T^*. Finally, by introducing an isotropic bulk modulus for the amorphous phase, it is found that e-C has a much lower compressibility than i-C*, enhancing the distinguishability among the two low-coordinated forms of α-C.

I. INTRODUCTION

Amorphous materials have interested scientists for years because of their complexity and, sometimes, quite unexpected properties. A large effort has been devoted to understanding the microscopic origin of such properties, of tremendous variation, ranging from mechanical and elastic characteristics to electronic and optical behavior. Among these materials, amorphous forms of carbon hold a special and unique position. The ability of carbon to display various coordinations under normal temperature and pressure conditions leads to a very diverse range of disordered structures. It is necessary to distinguish, from the beginning, between quasi-two-dimensional, graphitelike networks with a high degree of intermediate-range order, such as glassy carbon, and the truly amorphous carbon structures which are seemingly much more disordered, since medium-range order is rather absent,[1] as we shall discuss below.

The classification of amorphous carbons (α-C) is usually based on the examination of their macroscopic properties, such as density, hardness, and optical transparency. The next step is to attempt to infer their microscopic nature, either directly from experimental observations or by constructing models that are capable of explaining the macroscopic properties. The fundamental issue to be resolved is the relative ratio of threefold, graphitelike (sp^2) local bonding geometries to tetrahedrally bonded (sp^3) sites. This ratio is believed to largely control the properties of α-C films, although sometimes rather simplistic arguments and proposals are made in order to interpret the undoubtedly firm macroscopic observations. We might also add that the determination of the sp^2:sp^3 ratio suffers from uncertainties in the experimental techniques which lead to controversial results.

It is by now well established that the nature of α-C films depends on the preparation method and on the concentration of hydrogen in the sample.[2] We can, therefore, categorize amorphous carbons into basically three classes. Evaporated amorphous carbon (e-C), which is produced by evaporation in an electron beam or carbon arc, has graphitic macroscopic characteristics since it is black and soft with a density of ~ 2.0 g cm^{-3}, somewhat lower than that of graphite (2.27 g cm^{-3}), and has an optical gap of ~ 0.5 eV.[2] The essentially graphitic nature of e-C is furthermore microscopically established by the domination of sp^2 local bonding. At present, there is a consensus that the majority of atoms are sp^2 hybrids, as experimental evidence,[1,3–5] confirmed by theoretical calculations,[6–8] suggests. The reported concentration of sp^3 sites ranges from 5 to ~ 50 %, but the larger proportions[3] (50%) might not be that accurate. More reliable estimates would range from ~ 10 to ~ 30 %. The concentration of sp^3 sites has also been found to depend on temperature. Near-edge (NEXAFS) and extended (EXAFS) x-ray-absorption fine-structure studies,[9] indicate that the sp^2 fraction ranges from 60%, at $T = 30$ °C, to 90%, at $T = 1050$ °C.

Hydrogenated amorphous carbon (α-C:H) films form a second class of materials. They are usually produced by plasma deposition[10] or ion-beam deposition[11] of gaseous hydrocarbons. Hydrogen concentration in these films ranges from 20 to 60 % and it is found to markedly affect their properties.[12] Indeed, as hydrogen content increases,

two competing characteristics appear. At first, the material shows certain diamondlike properties, such as a large optical gap which reaches ~ 2.5 eV. This is attributed to the consequent increase of sp^3 sites in the samples, as it is directly probed by nuclear-magnetic-resonance (NMR) methods.[13] At the same time, however, the films become softer with densities less than 1.8 g cm^{-3}. This behavior may occur because of the development of polymeric, soft regions which deteriorate the hardness of the material. It is also found that the number of carbon neighbors to other carbon atoms changes only slightly with increasing hydrogen content, and that quaternary carbon (a carbon atom bonded to four other carbon atoms) is absent from α-C:H, as NMR studies show.[14] Thus, all sp^3 carbon atoms are bonded to one or two hydrogen atoms.

The third class of materials, which could more appropriately be classified as diamondlike amorphous carbon, consists of ion-beam-deposited carbon films (*i*-C), without or with a minimal concentration of hydrogen. The ion-assisted deposition techniques include sputtering, magnetron sputtering, ion deposition, vacuum-arc deposition, etc. These films are macroscopically truly diamondlike because they exhibit optical transparency and low conductivity, along with high hardness and density (reaching ~ 2.9 g cm^{-3}, compared to 3.51 g cm^{-3} for diamond).[15,16] Not surprisingly, therefore, diamondlike films have attracted much of the current interest in amorphous carbon and they are highly suitable for hard, transparent coating materials in microelectronics as well as in mechanical applications.

However, contrary to *e*-C, and despite their well-documented macroscopic properties, the microscopic nature of diamondlike films remains controversial. The central issue that is strongly debated is the extent of fourfold sp^3 local bonding in *i*-C, and how this affects its mechanical properties (hardness) and its optical properties (energy gap). In fact, the absence of hydrogen from the amorphous network offers the possibility for an exciting and appealing proposal. If the vast majority of carbon sites in *i*-C are sp^3 hybrids, then we have an amorphous carbon structure described by a tetrahedral continuous random network (CRN) model, in analogy with amorphous silicon or germanium. In a CRN model, such as that proposed by Polk,[17,18] each atom has four nearest neighbors arranged in a tetrahedral geometry, and so for a tetrahedral α-C structure, bond lengths and bond angles would be distributed about their crystalline diamond values. In such a predominantly tetrahedral network then, any threefold-coordinated atoms most likely should be viewed as intrinsic defects, something analogous to the dangling-bond defect in α-Si, and not as part of the inherent amorphous disorder, since they would be isolated.

Hints for a large fraction of sp^3 sites in *i*-C were given by the work of Zelez,[15] who produced nearly hydrogen-free carbon films with high density, 2.8 g cm^{-3}, and an optical gap of ~ 3.0 eV. Actually, the first estimation of the proportion of sp^3 sites in ion-sputtered films was made by Savvides[19] from an analysis of optical and transmission electron-energy-loss spectroscopy (EELS) measurements. He inferred a large fraction of sp^3 sites, ranging from 40 to 75 %, by extrapolating from the sum rule on the complex dielectric function of α-C, but his films had a gap more like that in *e*-C (0.4–0.8 eV). This procedure for determining the relative fraction of sp^3 and sp^2 sites from the dielectric function, however, was later questioned by Gao *et al.*,[5] who, instead, by using (*e*, 2*e*) spectroscopy, found that the sp^2 concentration in *i*-C is similar to that in *e*-C, ranging from 75 to 100 %. The difference between the two materials, according to these authors, lies in the π-electron spectral density, which for *e*-C is similar to graphite, while for *i*-C shows significant *s*-*p* hybridization, resulting from the twisting of sp^2-bonded sheets. The whole picture got more controversial after recent electron-diffraction[20] and neutron-scattering[21] studies of *i*-C, grown using a filtered vacuum-arc technique, which propose the existence of an almost entirely tetrahedral α-C network.

Obviously, the suggestion for such a tetrahedral α-C structure immediately raises the question of its stability. This, from the point of view of experiment, requires the thermal annealing of the reported structures. From the point of view of theory, it requires the study of the energetics of diamondlike films and the comparison with the energetics of *e*-C samples. Of particular interest, besides the estimation of the total energies of these α-C structures, is the examination of the energetics of local bonding geometries (sp^2 vs sp^3), in order to gain insight into the problem at hand. Such an analysis would, in addition, serve as a complement to the structural probing given by experiment, and would reveal the interrelation between structural and energy properties of α-C.

In this paper, I present detailed simulations of both forms of unhydrogenated α-C (*e*-C and *i*-C), with the purpose of establishing such a connection among the structural characteristics and the energetics of the system. A shorter report of these simulations, primarily on the energetics of the diamondlike phases, has recently been published.[22] By systematically studying the variations of density with temperature, along with the energetics of local geometries, while at the same time monitoring the structural changes with radial-distribution-function (RDF) and structure-factor $S(k)$ analyses, we are able to obtain a comprehensive picture and explain the controversial experimental reports on *i*-C. The next section deals with the methodology on which the simulations are based. Section III gives the results and their discussion, and the paper is concluded in Sec. IV.

II. METHODOLOGY

Contrary to random network models[8] which have been developed in order to understand the microscopic properties of α-C, the present approach is a type of direct simulation, avoiding any experimental inputs and *a priori* assumptions about the network topology. Of course, modeling the energetics in such a disordered system is a difficult task, because of the variety of bonding possibilities which might be displayed by carbon. A reliable description of the interatomic interactions and energetics is provided by using the empirical interatomic potential for carbon proposed by Tersoff.[6] The parameters in this

potential were chosen by fitting the cohesive energies of carbon polytypes (values from the work of Yin and Cohen[23] were used for the hypothetical phases), along with the lattice constant and bulk modulus of diamond. The potential has been well tested[6] by calculating the elastic constants and phonon frequencies, defect energies, and migration barriers in diamond and graphite. It is especially suited to the present simulations because it describes the small energy difference (~ 0.03 eV) between graphite and diamond very well, being thus able to distinguish among different carbon environments (sp^2 vs sp^3) in disordered systems.[24]

Necessarily, this approach is less accurate than quantum-mechanical calculations. However, it has the advantage of great statistical precision (since it allows extensive sampling in the configuration space), and it makes the simulations tractable by allowing the use of large cells to model the amorphous network. In contrast, *ab initio* molecular-dynamics methods are so numerically intensive that they are restricted to short simulation times and small numbers of atoms.

What makes, however, the use of the empirical-potential approach so desirable in this problem, is the special analysis applicable to our results. Indeed, the key element in the present approach to the energetics of the amorphous system is the decomposition of the cohesive energy of the sample among the atoms, as it is explicitly specified in the definition of the interatomic potential used here.[6] In this scheme the energy is modeled as a sum of pairlike interactions, but the coefficient of the attractive term (playing the role of a bond order) depends on the local environment, giving a many-body potential. The functional form of the energy E is given by

$$E=\sum_i E_i=\frac{1}{2}\sum_{i\neq j} V_{ij} ,$$

$$V_{ij}=f_c(r_{ij})[f_R(r_{ij})+b_{ij}f_A(r_{ij})] ,$$

$$f_R(r)=A\exp(-\lambda_1 r) ,$$

$$f_A(r)=-B\exp(-\lambda_2 r) ,$$

where $f_c(r)$ is a cutoff function limiting the range of the potential between only first neighbors and b_{ij} is the bond-order function. Details about these terms can be found elsewhere.[25] In the partitioning scheme, the interaction energy V_{ij} between atoms i and j is equally divided among them. A site energy E_i is then the sum of such contributions to the reference atom from its nearest neighbors. Such a decomposition of the total energy, although not unique, can be made in practice, and it has already given valuable information on atomic-scale properties of α-Si (Ref. 26) and alloy-semiconductor surfaces.[27] Such an analysis would be impossible in an *ab initio* total-energy calculation.

For the purposes of this investigation, amorphous carbon structures are computer generated by rapid quenching of liquid carbon under various pressures. For e-C samples, low pressures of 1–10 kbars are used in order to prevent the formation of unphysically large voids. For diamondlike i-C samples we use high (1–2 Mbars) pressures. Although typically α-C is made by vapor deposition, the above procedure is quite relevant to experimental situations. Indeed, it closely resembles the various ion-assisted deposition processes (even though it is not directly related to their actual kinetics), since it is believed[11,20] that during deposition the incoming ions with high kinetic energies produce localized melting and subsequent rapid quenching of a small region.

I use cubic computational cells of 216 atoms with periodic boundary conditions. The formation of the amorphous networks and the investigation of their properties is simulated using a continuous-space Monte Carlo (MC) algorithm in the constant pressure-temperature (N, P, T) ensemble. This is advantageous because it allows volume and density fluctuations and avoids the *a priori* fixing of the density (as done in previous simulations of α-C with *ab initio* molecular dynamics).[7] Such fixing is undesirable here because it is crucial that any changes in density due to thermal annealing be described accurately. To form the amorphous structure one begins with a well-equilibrated liquid at temperatures ranging from ~ 6000 to ~ 9000 K, depending on the applied pressure. Note that with increasing pressure, high temperatures are needed, because the diamond–liquid carbon boundary in the phase diagram of carbon[28] has a positive slope, as recent simulations show.[29,24(b)] The melt is then quenched at inverse rates of ~ 8 MC steps/atom K down to 300 K, where the pressure is removed and the sample densities are equilibrated.

III. RESULTS AND DISCUSSION

In this section, a thorough exposition of structural and energy properties of evaporated (e-C) and diamondlike amorphous carbon (i-C) is given. From the analysis, outlined in the previous section, it naturally follows why sp^2 sites are predominant in e-C and it is demonstrated that two dense, diamondlike phases exist, distinguished from each other and from e-C.

We begin by considering the properties of e-C, which is formed at low pressures and considered to be the typical form of α-C. Although, as mentioned in the introduction, the short-range order (SRO) of this material is well established (that is, graphitelike sp^2 in nature), the degree of medium-range order (MRO) is still debated. Previous interpretations of experimental work and theoretical models[2,30] were suggesting a high degree of MRO, with the sp^2 sites participating in ordered graphitelike sixfold rings (π-bonded clusters) embedded in a sp^3-bonded matrix.[31] However, this proposition is not supported by the recent experimental results of Li and Lannin,[1] who found no evidence for a significant fraction of sixfold rings. As was pointed out by these authors, their structure is consistent with the predictions of the empirical model of Tersoff,[6] which is also used here. Indeed, the present simulations confirm the small fraction of planar sixfold rings, while the presence of five- and seven-atom rings, as well as of larger rings, is significant, in agreement with recent molecular-dynamics (MD) simulations[32] (using the Tersoff potential, too).

It seems then, that real e-C is much more disordered than predicted in the model of Robertson and O'Reilly[31]

and that MRO is not significant. To be fair, however, we should point out that the empirical model of Tersoff is short ranged and that the absence of longer-ranged forces might distort the MRO. Nevertheless, the agreement between the predictions of this model and the experimental results[1] cannot be considered as fortuitous. The comparison of the experimental structure factor $S(k)$, see Ref. 1, and the theoretical one, shown in Fig. 1(a), ensures that. The agreement is excellent even for low-k values. In addition, the presence of five- and seven-atom rings, and a distorted nonplanar character of sp^2 sites, is also found in the *ab initio* molecular-dynamics simulations of Galli *et al.*,[7] which by virtue of their nature include long-ranged forces and thus should be able to treat MRO. In any case, the question of MRO might need further consideration, but this does not affect our discussion because the total energy of the system, arising from the arrangement of σ bonds in the amorphous network, depends on short-ranged factors, such as bond length and bond angle variations.

By decomposing the total energy of the system (~ 6.95 eV/atom, on the average) into site energies, as explained above, we obtain the distributions of atom energies by averaging over $\sim 10\,000$ MC steps/atom at 300 K. These are shown in Fig. 2(a) for a typical sample, consisting of $\sim 88\%$ sp^2 atoms and having density of $\sim 56\%$ that of diamond. $P(E)$ is the probability of finding an atom with energy E. As expected, the solid line (total distribution) has a low-energy cutoff at about the crystal energy of

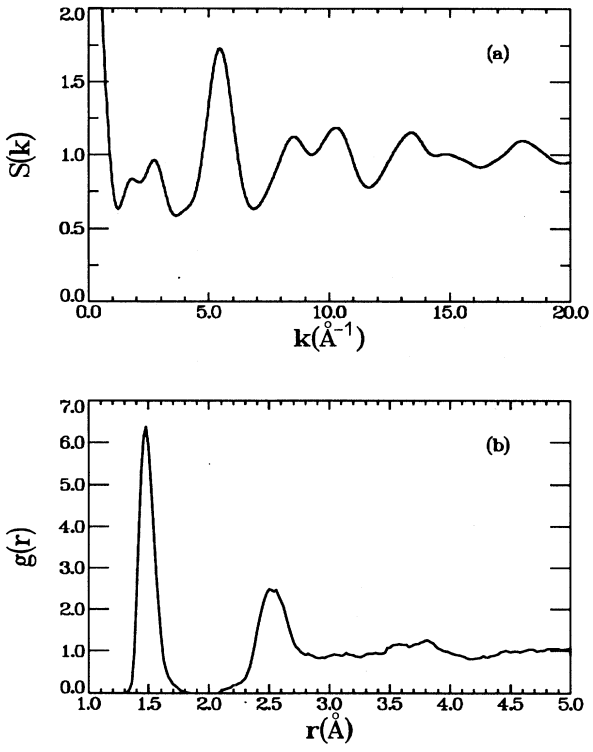

FIG. 1. (a) Calculated structure factor $S(k)$ of e-C. (b) Calculated radial distribution function of e-C (arbitrary normalization).

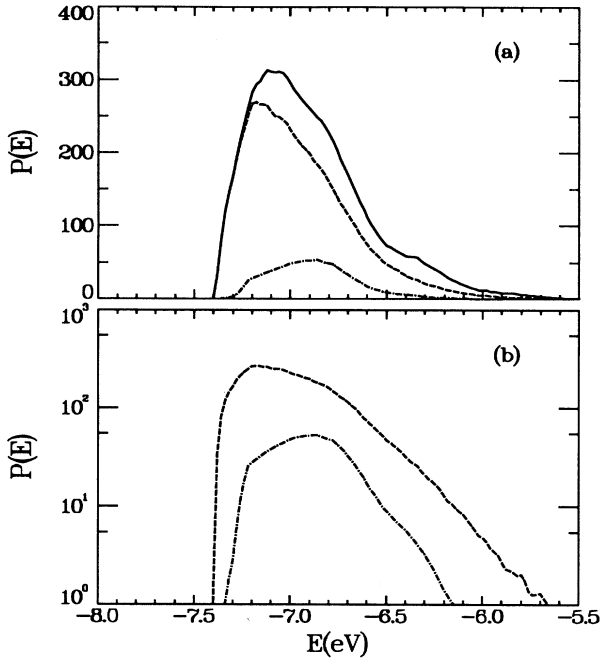

FIG. 2. (a) Distributions $P(E)$ of atom energies in e-C at 300 K. Solid line denotes the total distribution. Dashed and dot-dashed lines are projected distributions for threefold- and fourfold-coordinated atoms, respectively. (b) Same data on a logarithmic scale (solid line is omitted).

~ 7.4 eV. (Remember that the experimental values for the cohesive energy of graphite and diamond are -7.374 and -7.349 eV/atom, respectively.[23]) The majority of atoms have energies at about -7.1 eV, and then there is a high-energy tail of considerable energy range (~ 2 eV), which obviously contains the energies of weakly bonded atoms with severely strained bonds and large angle distortions. Actually the tail also contains in most samples a very small peak at ~ -5.10 eV (not shown here), which arises from few twofold-coordinated atoms. These must be viewed as defects in the amorphous network with a formation energy of ~ 2 eV, and can be easily eliminated by annealing, as we shall discuss below.

In order to define the coordination of each atom, we count the number of neighbors within ~ 1.8 Å, the position of the first minimum in the radial distribution function $g(r)$, shown in Fig. 1(b). By doing that, we can decompose the total contribution to the $P(E)$ into partial contributions from individual atoms according to their coordination. This decomposition (we ignore the small contribution from twofold sites) in depicted by the broken lines in Fig. 2(a). It is evident that the major contribution to the $P(E)$ originates from the threefold sites, which have a peak in their energy at ~ -7.2 eV. The distribution of fourfold atoms, on the other hand, has a peak at ~ -6.85 eV, significantly higher (~ 0.35 eV) than the threefold peak. Thus, we have arrived at a result concerning the local geometries in e-C, which has probably been speculated but not explicitly shown before. It is nicely demonstrated that threefold sites are the energetically favorable geometries in the amorphous network,

and that is why they are by far more numerous.

One could argue, of course, that this result is expected because graphite has a slightly lower cohesive energy than diamond, at low pressures. Two observations, however, make this argument not as easily applicable when dealing with the amorphous phase. As we discussed above, it seems that MRO is insignificant in *e*-C and therefore we should not characterize it as a disordered form of graphite. (In contrast, glassy carbon conforms to that, because it has been shown[33] that two-dimensional graphitelike order exists in this material.) Thus, threefold geometries in *e*-C are only locally graphitelike. In addition, the predominance of sp^2 bonding to such an extent is not justified by the small energy difference (~ 0.03 eV/atom) between graphite and diamond. These points suggest that the reference to the two crystalline phases does not solely determine the energetics of the disordered system, but that an additional factor plays a crucial role, namely, the degree of structural disorder in the immediate neighborhood of individual atoms. For example, strained bonds, nonplanar character of threefold sites, and large angle distortions strongly influence the energetics of local geometries. In fact, the substantial energy difference of ~ 0.3 eV among threefold and fourfold atoms (compared to only 0.03 eV in the crystal) means that, on average, the sp^3 units are more distorted than the sp^2 configurations. A similar conclusion, based on structural analysis, is reached by the MD simulations of Galli *et al.*[7]

Additional insight into the properties of *e*-C is gained by looking at the distributions of atom energies on a logarithmic scale, shown in Fig. 2(b). It is obvious that the high-energy tail of the threefold sites, which are the vast majority of atoms in the sample, closely obeys an exponential Maxwell-Boltzmann distribution. A similar behavior of local geometries has also been observed in previous simulations of α-Si.[26] Interestingly, analysis of the slope gives an effective temperature T^* of about 2600 K, which is much higher than the 300 K temperature used in averaging for the atom energies. We identify with T^* the "glass transition temperature" of the sample, which signifies the onset of the transition from liquidlike states to a supercooled liquid, i.e., to a glass. At T^* substantial atom motion ceases and the undercooled liquid becomes effectively a solid. Mobility below T^* mainly involves bond switching, rather than actual diffusion of atoms. (Actually T^* refers to the slope of the total distribution which, in any case, is mostly contributed by threefold atoms.) Analyzing other samples gives similar values for T^*, which is a slightly monotonically increasing function of quench rate.

The distribution of fourfold atoms also exhibits this exponential behavior. The extracted effective temperature T_4^* of ~ 1800 K, however, is much lower than T^*. This means that the fourfold geometries are, on average, still mobile down to T_4^* (analysis of other samples indicates that T_4^* could be even lower, close to 1500 K), without excluding the possibility that the weakly bonded fourfold atoms can be mobile, through bond switching, at even lower temperatures. Similarly, although the statistics for the few twofold defects are rather poor, we can also infer an effective temperature T_2^* of ~ 700 K. This variation in the values of effective temperatures for differently coordinated atoms makes it tempting to suggest that the defects and many of the sp^3 sites (especially the weakly bonded ones) tend to anneal in the appropriate temperature range. Thus, this theory can very nicely explain the experimental observations[9] for an increasing graphitic character or *e*-C as the temperature is raised (the sp^2 fraction ranges from 60% at $T=30\,^\circ$C, to 90% at $T=1050\,^\circ$C). Indeed, as we have checked, the defects disappear with annealing above 800 K, while the weakly bonded sp^3 sites are progressively eliminated by annealing above ~ 1400 K. Note, when comparing with the experimental values, that the effective temperatures, as inferred here, could be somewhat overestimated, as it is the melting temperature of C with the present potential.[6]

Having shown the value and applicability of the partitioning scheme, we now wish to study the dense or diamondlike phase of α-C. I have generated many samples with the quenching procedure previously described. Various properties are summarized in Table I, along with properties of *e*-C for ready comparison. The key point in the process of quenching to room temperature under applied high pressure is that the system is driven inside the zone, in the phase diagram of carbon,[28] where diamond is the stable phase. As it is claimed by McKenzie, Muller, and Pailthorpe[20] in vacuum-arc growth there exist such conditions (low T, high P), so that it would be possible to grow an entirely tetrahedral material, characterized as an amorphous form of diamond, and that this method is fundamentally different from the metastable growth of crystalline diamond by chemical-vapor deposition under reduced pressure. According to these authors, an electron-diffraction study of vacuum-arc-deposited films showed that the produced material was almost completely tetrahedral, with coordination number exceeding 3.9, and had high density of about 2.9 g cm^{-3}.

Our simulations indicate that after equilibration at 300

TABLE I. Calculated properties (averages over approximately five samples) of the "as-quenched" (*i*-C) and annealed (*i*-C*) diamondlike phases and of evaporated amorphous carbon (*e*-C) at 300 K; positions of peaks in the $g(r)$, most probable bond angles, density ρ, coordination z, total energy per atom, positions of peaks in the decomposed $P(E)$, and isotropic bulk modulus B_0. Also given for comparison are corresponding numbers for graphite (G) and diamond (D).

Property	*i*-C	*i*-C*	*e*-C	G	D
r_1 (Å)	1.53	1.48	1.47	1.46	1.54
r_2 (Å)	2.52	2.52	2.53	2.53	2.52
θ (deg)	110.9	116.7	118.7	120	109.5
ρ (g cm^{-3})	3.2	2.9	2.0	2.27	3.51
z	3.70	3.25	3.1	3.0	4.0
$-E$ (eV)	6.75	~ 6.95	~ 6.95	7.37	7.35
$-E_3$ (eV)	7.12	7.2	7.2		
$-E_4$ (eV)	6.8	6.85	6.85		
B_0 (Mbars)	4.2	3.9	2.3	2.8[a]	4.4[b]

[a]Experimental value. See Ref. 23.
[b]With Tersoff's potential.

K, the "as-quenched" (in analogy to "as-deposited") samples indeed can have high densities reaching 3.2 g cm^{-3}, or 90% that of diamond, even higher than that given in Ref. 20. The coordination number, however, is about 3.6–3.7 on the average, and it does not exceed 3.8, even at the highest pressure considered (2 Mbars). Quenching at higher pressures is possibly meaningless, since the experimentally reported[20] compressive stresses, which are responsible for promoting the sp^3 fraction, do not exceed ~6 GPa (=60 kbars), and because it was found that incident-ion energies beyond some value tend to reduce the sp^3 fraction.[20,32] Of course direct comparison of the pressure values among experiment and theory is not proper because the actual kinetics are not related. Instead, trends should be compared. Anyway, our results suggest that the formation of an entirely sp^3-bonded network is rather unlikely. This is at odds with the proposition made in Ref. 20, based on electron-diffraction studies, although neutron-scattering studies of the same material report a coordination number of ~3.8, with a significant fraction of atoms having a connectivity characteristic of trigonal bonding.[21]

A similar analysis of the energetics, as done for *e*-C, is now applied to *i*-C. Figure 3(a) shows the energy distributions for a typical, equilibrated, "as-quenched" sample. These are quite broad, indicating that there is considerable amount of strain in the cell, in agreement with the experimental observations[20] that the localized melting and rapid quenching of a small region leaves it in a stressed state. The major contribution to the $P(E)$ arises from fourfold atoms, as expected, since they are more numerous. The energies of these atoms, however, peak at ~ −6.8 eV, significantly higher than the peak of the threefold distribution (~ −7.1 eV). Evidently, the process of rapid freezing traps the sp^3 sites into local-energy minima, well above the more energetically stable state of the threefold atoms, even though the formation of tetrahedral atoms is favored under conditions of high pressure, because this lowers their enthalpy. The total energy of this dense and high-coordinated phase is, on the average, about −6.75 eV/atom, significantly higher than the total energy of an *e*-C sample.

These observations unavoidably lead to the question of stability of the "as-quenched" structures. Mechanical applications of diamondlike films demand thermal stability at high temperatures, but I am not aware of any annealing study of the vacuum-arc-deposited films.[20,21] Here, we address the stability issue by annealing the quenched samples at successively higher temperatures and then cooling them to 300 K. Annealing is continued at the desired temperature until no more changes are observed. This means more than 100 000 MC steps/atoms, especially at lower temperatures where diffusion is slow. The results of the annealing process are entered in Table I, while the changes in the most crucial parameters, coordination and macroscopic density, are portrayed in Figs. 4(a) and 4(b).

We first discuss the changes in coordination. The results shown in Fig. 4(a) are for the sample where the highest coordination (~3.8) was achieved. The reduction in coordination z is dramatic. Already at 1200 K z becomes ~3.4, while at 2500 K, z drops to less than 3.2. The smooth transition to a new sp^2-rich phase (*i*-C*) is obvious. A significant energy gain of ~0.2 eV/atom follows the annealing process, indicating that the "as-quenched" configurations are in a metastable state. This "phase" change is also clearly observable in the energy distributions of the annealed sample, which are shown in Fig. 3(b). The height of the fourfold distribution is drastically decreased, while the opposite is true for the threefold distribution. In addition, the width of both distributions has been shrunk, indicating that the excessive strain present in the "as-quenched" phase has been now partly relieved. The positions of the peaks of both distributions are very similar to those in the *e*-C samples. Their total energy is also very close. The structural changes are similarly evident from a comparison of the radial distribution functions $g(r)$ of the *i*-C and *i*-C* phases, which are shown in Fig. 5. Both the first- and the second-neighbor peaks, which are quite broad for *i*-C, are now narrowed and sharpened, while bond lengths drastically

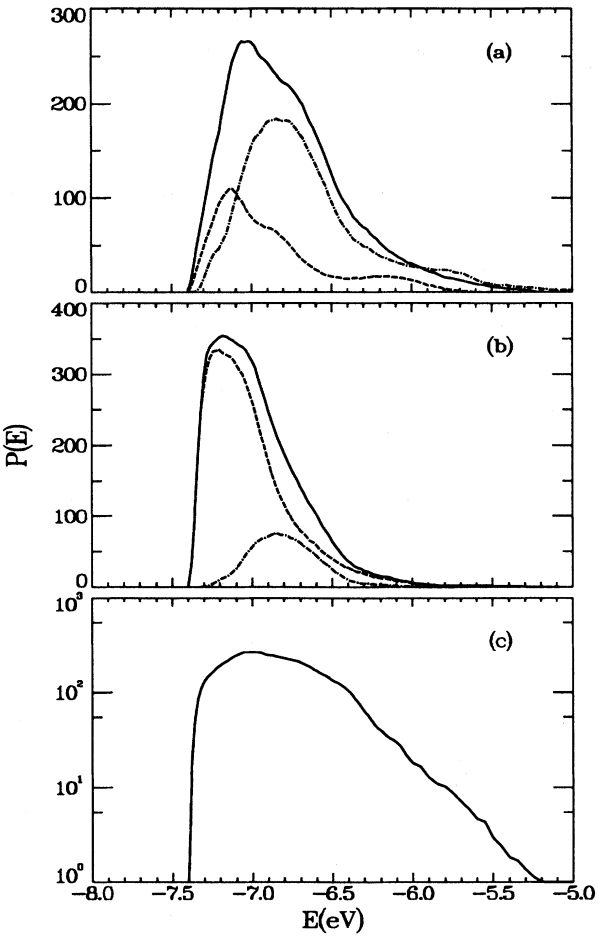

FIG. 3. Distributions $P(E)$ of atom energies in diamondlike α-C at 300 K. Solid line denotes the total distribution. Dashed and dot-dashed lines are projected distributions for threefold- and fourfold-coordinated atoms, respectively. (a) $P(E)$ for *i*-C. (b) $P(E)$ for *i*-C*. (c) The total $P(E)$ for *i*-C, shown in (a), on a logarithmic scale.

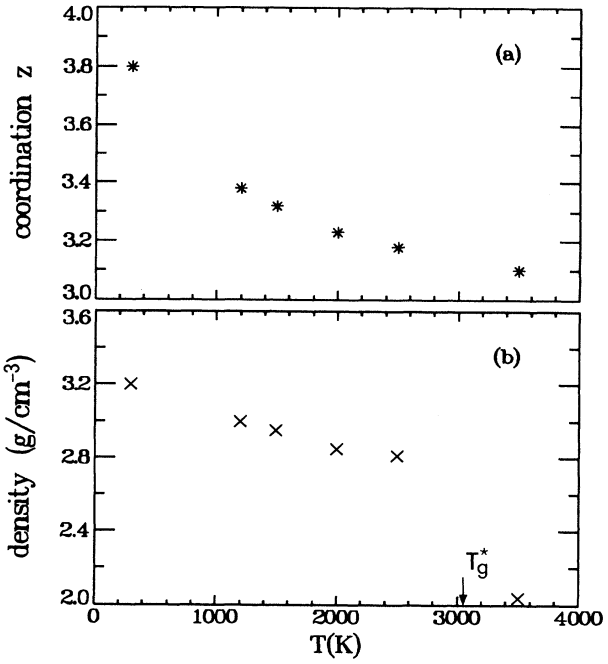

FIG. 4. (a) Coordination z vs annealing temperature for an i-C sample. (b) Density of the sample vs annealing temperature. Also shown is the "glass transition temperature" T^*.

shift from diamondlike (1.53 Å) down to graphitelike (1.48) values.

In order to unravel the mechanism for the elimination of many sp^3 sites, it is worth a close look at the geometries of fourfold atoms before annealing. We find that a large number of these atoms possess extremely strained and thereby weak bonds, as is confirmed by examining the $g(r)$ of the i-C sample in Fig. 5. Indeed, the broad first peak of the $g(r)$ has a tail containing stretched bonds with lengths up to ~ 1.9 Å. In addition, large angle distortions occur in this sample, as is indicated by the width of the bond angle distribution, shown in Fig. 6. Then, fourfold atoms containing such a weak bond and large angle deviations are weakly bonded, with energies lying in the tail of the distribution in Fig. 3(a). This suggests that thermal annealing could supply the necessary energy to a weakly bonded fourfold atom, in order to overcome the potential barrier and move out of the local well where it was trapped. Consequently, the atom lowers its energy by transferring the weak bond to the neighboring cluster of atoms, so becoming a threefold coordinated site, and by relaxing the remaining bond angles and lengths to relieve strain. Such a mechanism involves a cluster of relatively few atoms, and is therefore of local nature. The resulting threefold sites, as well as the already existing are distorted sp^2 units. This is confirmed by comparing the bond angle distribution of an i-C* sample with that of an e-C sample. As mentioned above, the distorted, nonplanar character of sp^2 sites even in e-C has also been supported by experiment[1] and *ab initio* MD simulations.[7]

The other important ingredient in the characterization of these amorphous structures is their macroscopic density. Possibly the most remarkable finding of the present simulations concerns the density of annealed samples. Figure 4(b) nicely shows that, despite the drastic reduction of sp^3 sites by annealing at the designated temperatures, the density remains high (~ 2.9 g cm^{-3} on the average). Annealing at 2000 K reduces ρ to 2.85 g cm^{-3}, and at 2500 K it becomes 2.81 g cm^{-3} ($\sim 80\%$ of the density of diamond). Therefore, while clearly there is a transition to an sp^2-rich phase, the annealed samples remain dense and diamondlike and we cannot speak about graphitization. Note also that the densities we give here for i-C* are very close to those reported for the vacuum-arc-deposited films.

This remarkable behavior of density as a function of annealing temperature can be nicely explained by resorting to the same kind of approach that was applied to the e-C samples. We first note that density is a macroscopic property, that is a function of all atomic coordinates in the sample and not just of local nature. This suggests

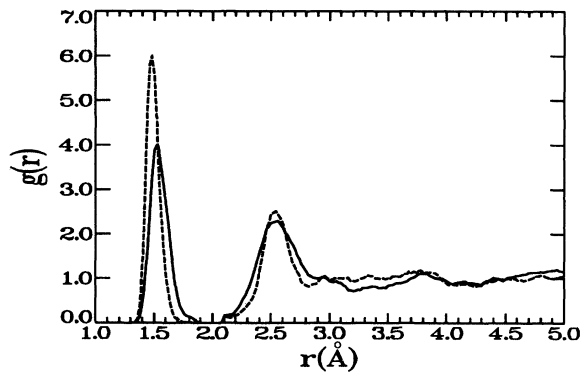

FIG. 5. Calculated radial distribution functions for the two diamondlike phases (arbitrary normalization). Solid line: "as-quenched" phase. Dashed line: annealed phase.

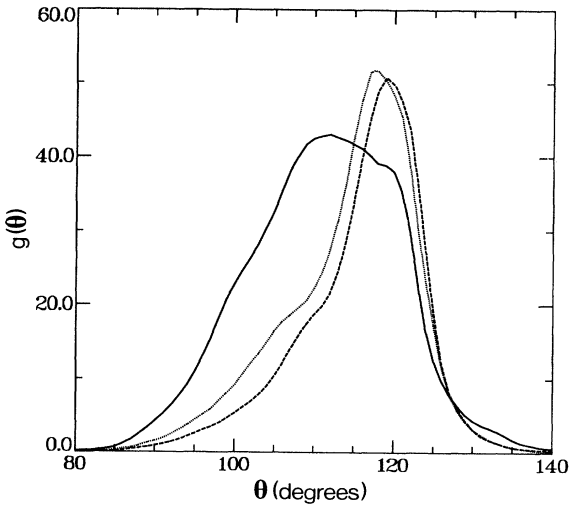

FIG. 6. Bond angle distributions (arbitrary normalization). Solid line, "as-quenched" diamondlike phase (i-C); dashed, annealed diamondlike phase (i-C*); dotted, evaporated α-C (e-C).

that, contrary to the annealing of weak sp^2 sites studied above (which only involved appropriate relaxations of the neighboring cluster of atoms), we might need to completely rearrange the amorphous network in order to reduce the diamondlike densities down to graphitic values (and even lower). To achieve this, one must anneal the samples above the "glass transition temperature" T^* as is immediately suggested by the mere definition of T^* given previously. Here, we should rather look at the high-energy tail of the total distribution $P(E)$ of the "as-quenched" sample in Fig. 3(a). The same data on a logarithmic scale are shown in Fig. 3(c). Analysis of the slope gives an effective T^* of ~ 3000 K. As a check, the temperature at which self-diffusion becomes negligible (evident from the limiting behavior in the atomic mean-square displacement), either during quenching or during annealing, is fairly close to T^*. We also note that the inferred T^* for i-C seems to be somewhat higher (analysis of other samples gives consistently similar values) than the respective effective temperatures of e-C. This might be possible since with increasing pressure, as argued above, the melting point is elevated (we have a positive slope of the diamond–liquid carbon phase boundary), and along with it the glass transition point does the same.

A look back to Fig. 4 indeed confirms the expected result. Annealing at 3500 K induces an abrupt drop of density from ~ 2.8 to ~ 2.0 g cm^{-3}, which is a characteristic value for e-C. There is also a small and smooth change in coordination to ~ 3.1. Let us recall from the above discussion that below T^* the amorphous network is essentially frozen. Annealing of weak sp^3 sites at temperatures less than T^*, followed by a small change in density, occurs only because it involves bond switching rather than actual diffusion of the atoms. We also suggest that, since T^* might be overestimated with the present potential, effective annealing of sp^3 sites could be observable at even lower temperatures than studied here (< 1200 K), which are presumably accessible by experiment.

We are now in a position to compare our findings with the conflicting descriptions of the diamondlike phase given by experiment. What is, at the first look, a surprising finding in the present simulations, is the existence of a diamondlike phase (the annealed i-C* phase) with high density but a low coordination number. This proposition, however, is not so radical and it is supported by the (e, $2e$) spectroscopy data[5] in ion-sputtered films, which indicated low sp^3 concentration but large optical gaps. This was attributed to significant s-p hybridization resulting from the twisting of sp^2 graphitic planes and the loss of mirror plane symmetry. Interestingly, a recent Raman scattering study[34] of α-C films, grown by different techniques, finds that arc-evaporated films are structurally "less graphitic" than ion-sputtered films, in contradiction with the e-$2e$ data,[5] and despite the fact that e-C films have smaller energy gaps. Although the microstructural differences between evaporated and ion-sputtered films are sensitive and important, and need further consideration, the Raman study[34] does not alter the main conclusion of this work, that a diamondlike phase can be predominantly sp^2-like, but rather enhances it. I would add here, that sometimes the difference in density between evaporated and ion-sputtered films is not reported by the experimental work.[5,34] This makes things a little confusing because macroscopic density should be the main criterion (besides the optical gap) to distinguish among diamondlike (hydrogen-free) and evaporated films.

Further support for a low-coordinated diamondlike phase is provided by a theoretical model of Tamor and Wu.[35] They have constructed a "defected graphite" model in which the presence of a small amount of disorder is able to induce localization of the π electrons and a "metal-insulator" transition. This disorder consists of randomly distributed defects, which can be a carbon vacancy, rehybridization, or interplanar links through sp^3 bonding. By using percolation arguments they show that no more than $\sim 8\%$ of sp^3 carbon (randomly distributed) is needed to induce π-electron localization. The model also predicts that interplanar links lead to a material with high density. Thus α-C films can exhibit diamondlike properties (insulating, transparent, and denser than graphite) and yet possess no actual diamondlike structure.

By no means, however, do the above arguments exclude the existence of a dense, diamondlike structure with high sp^3 concentration. Our finding that the as-quenched phase (i-C) contains a high percentage of sp^3 bonds is in accord with the reported structure of the filtered-vacuum-arc samples.[20,21] Interestingly, we find a higher density (~ 3.2 g cm^{-3}) compared to experiment (~ 2.9 g cm^{-3}), though the sp^3 concentration in the computer-generated samples ($\sim 70\%$) is lower than in the vacuum-arc samples ($> 90\%$). Possibly this difference is reflected in a rather high first peak in the calculated structure factor $S(k)$ of i-C, shown in Fig. 7(a), compared to the ex-

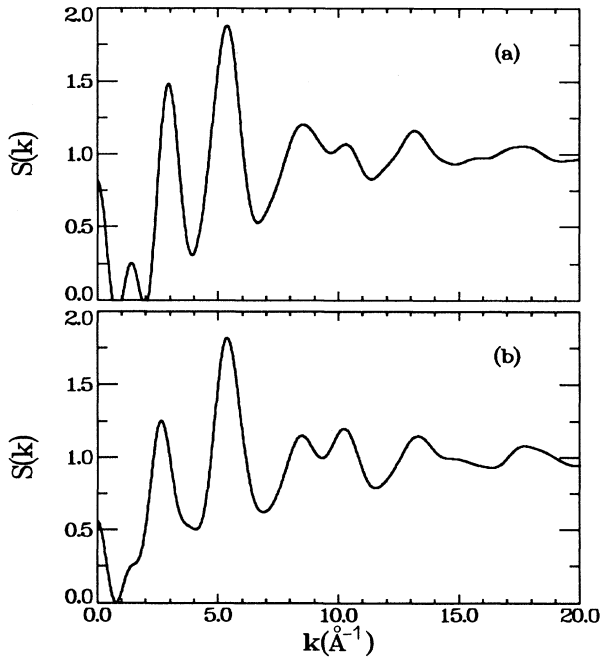

FIG. 7 (a) Calculated structure factor $S(k)$ of i-C. (b) Calculated $S(k)$ of the annealed (i-C*) phase.

perimentally (by neutron scattering)[21] determined structure factor (see Ref. 21). Also the minimum between the first and second peaks is deeper than in experiment. Otherwise, the position and the shape of the peaks are consistent with experiment.

The main point of this paper, nevertheless, is that such a high-coordinated dense structure is metastable to the sp^2-rich (i-C*) phase. Its structure factor, shown in Fig. 7(b), is distinguished from both the $S(k)$ of i-C, as well as from the $S(k)$ of e-C in Fig. 1(a). This metastability is different from the instability exhibited by diamond, under normal conditions, when only a small degree of disorder induces conversion to graphite (as ion-implantation studies indicate[36]), because in our case the stable structure retains the diamondlike density. It is also important to note that the large potential barrier for the conversion to the stable structure i-C*, at room temperature, might make it possible for the mostly fourfold-coordinated material to be realized for practical purposes. This will depend on the ability of a given deposition technique to produce and preserve the unstable fourfold geometries. To achieve this, one must minimize the available energy for transition to the more stable phase. Appropriate experimental conditions (such as low substrate temperature) seem to be able to preserve the sp^3 units.[16,20] For applications at higher temperatures, however, the metastability should be taken into account.

Our discussion of the diamondlike phase of unhydrogenated α-C will not be complete if we do not unquestionably differentiate between the low-coordinated diamondlike phase (i-C*) and the, as well low-coordinated structure of e-C. As seen from Table I, the two structures have practically identical energies. The structure factors $S(k)$, the radial distribution functions $g(r)$, and the bond angle distributions differ (see table and respective figures), but not so much. As is obvious from above, the stronger point and criterion of distinction is the macroscopic density. The next most crucial mechanical property for the characterization of α-C films is their hardness. Therefore, a nice way to enhance the distinguishability among e-C, and i-C* is to estimate some quantity which is relevant to hardness. Here, for convenience, we study the compressibility of our computer-generated samples. For this purpose, by analogy to the crystalline state and considering a uniform expansion (compression) of the system, we define an isotropic, equilibrium bulk modulus for the amorphous phase,

$$B_0 = V(d^2E/dV^2)_{V=V_0} ,$$

where V is the volume, V_0 the equilibrium volume, and E is the total energy of the cell. The calculated values of total energy vs lattice constant for three representative samples (e-C, i-C, and i-C*) are shown in Fig. 8. Such points (calculated for a number of different cells, about five for each case) are fitted to the Murnaghan's equation of state for solids,[37] yielding average values for B_0 which are listed in Table I. If we do a parabola fitting to the points we get similar results. The "as-quenched" phase has a B_0 ($\sim$4.2 Mbars) very close to that of diamond (4.4 Mbars). Actually, the sample shown in Fig. 8, with $\rho/\rho_d \simeq 90\%$ and $z \simeq 3.75$, has a B_0 of $\sim$4.55 Mbars,

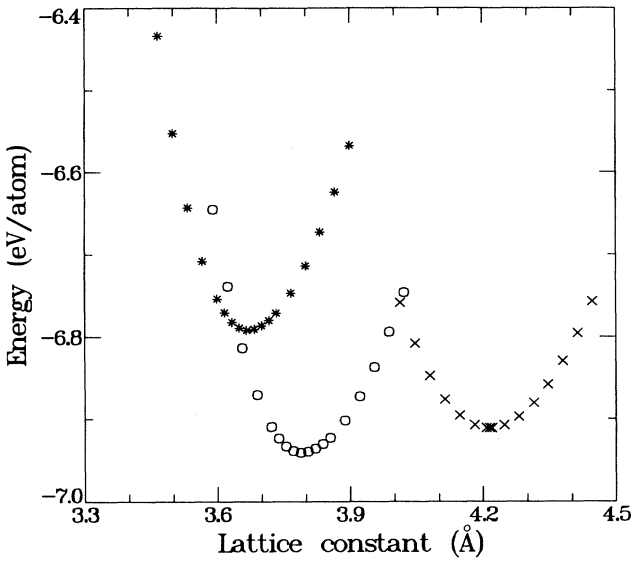

FIG. 8. Calculated values of total energy vs lattice constant for e-C (crosses), i-C (stars), and i-C* (open circles).

slightly higher than diamond's. This is consistent with reported values of hardnesses for i-C, ranging from 20 to 110 GPa, compared to 103 GPa for diamond.[38] The annealed stable phase i-C* has (on the average) a B_0 somewhat lower ($\sim$3.9 Mbars), but still comparable to diamond's (89%). On the other hand, e-C has a much lower value of B_0 (2.3 Mbars on the average). This nicely demonstrates the large difference in compressibility (and therefore hardness) between the two low-coordinated phases of α-C.

These results also demonstrate that α-C need not be predominantly sp^3 in order to have diamondlike hardness. The i-C* sample of Fig. 8 is only $\sim$25% sp^3 but still its rigidity approaches that of diamond. This finding seems to disagree with propositions that hardness in α-C films solely derive from the sp^3 component of the film's bonding. Robertson[39] recently suggested, assuming significant MRO, that in a two-phase model of α-C the sp^2 sites, which form planar-graphitic clusters, contribute no rigidity (but they control the electronic properties-energy gap), while the sp^3 matrix alone controls the rigidity. In this diamondlike phase (i-C*) however, we cannot speak of such a two-phase model since neither do the majority sp^2 sites form graphitic clusters, nor are the sp^3 sites the connective tissue around each cluster, but they are close to being randomly distributed (as a close examination of the neighbors of each atom shows). Instead, the hardness of the material should be attributed to its high density and the resulting compact, nonplanar and cross-linked arrangement of sp^2 bonding units. Interlinking through sp^3 sites also increases hardness. In this way both components of the films bonding contribute to rigidity. Therefore, densification and related existence of voids (size and distribution) should be an important ingredient in any model of rigidity, and not just the mean coordination of the network. Otherwise, the two low-coordinated phases (e-C and i-C*) would have similar hardnesses. That they differ is a result of the more open

structure of e-C, and indicates the existence of voids (a considerable fraction of small voids has been found by Li and Lannin[1]) in e-C and the absence, or the small number, of them in i-C*.

IV. CONCLUSIONS

Using a very efficient Monte Carlo algorithm, we have carried out extensive simulations, within the classical empirical-potential approach, in order to investigate the structure and energetics of the dense, diamondlike phases of α-C (i-C and i-C*), as well as of the low-density evaporated α-C (e-C), and make a comparative study of them. The interrelation between the structure, the energetics, and the stability of these phases is explored by applying a powerful and yet simple approach to the energetics of disordered systems, which is based on a total-energy-partitioning scheme.

For e-C, we have been able to demonstrate that threefold sites have lower energy than the fourfold atoms. They are less distorted, and, being the energetically favorable geometries in the amorphous network, they are by far more numerous. This cannot be anticipated from comparing graphite (the thermodynamically stable phase at normal conditions) to diamond, since threefold geometries are reminiscent of graphite only at the short-range level. Medium-range order seems not to be significant in e-C, as the nonplanar character of sp^2 sites and the absence of sixfold ring indicates, in agreement with the recent neutron-diffraction data of Li and Lannin.[1] By extracting the effective temperatures T^*, at which the atoms freeze in their lattice positions, we have also been able to explain the experimental observations[9] for an increasing graphitic character of e-C as the temperature is raised.

For diamondlike α-C, we have been able to reconcile and explain the conflicting descriptions given by recent experiments. The simulations demonstrate the existence of two distinctly different diamondlike structures. The "as-quenched," high-pressure phase exhibits high density with most of the atoms participating in sp^3 bonding, which is in accord with recently reported structures of filtered-vacuum-arc samples.[20,21] However, this is a metastable state. Upon annealing, it converts into another dense phase, but with the majority of atoms forming sp^2 units. Such a diamondlike phase is supported by (e, $2e$) spectroscopy data[5] in ion-sputtered films, and by the "defected graphite" model of Tamor and Wu.[35] A significant energy gain follows the annealing process. Specific mechanisms for these structural changes are explored, and the insensitivity of density to annealing is explained using the concept of the "glass transition temperature" T^*.

Finally, we have made an unambiguous distinction among the two low-coordinated phases of α-C in terms of their hardness, enhancing in this way their difference in density. For this purpose, we defined an isotropic, equilibrium bulk modulus for the amorphous phase, in analogy with the crystalline state. The two diamondlike phases (i-C and i-C*) have bulk moduli comparable to diamond's, while the bulk modulus of e-C is much lower, indicating the difference in compressibility and hardness of these materials.

[1] F. Li and J. S. Lannin, Phys. Rev. Lett. **65**, 1905 (1990).
[2] J. Robertson, Adv. Phys. **35**, 317 (1986).
[3] J. Kakinoki, K. Katada, T. Hanawa, and T. Ino, Acta Crystallogr. **13**, 171 (1960).
[4] B. T. Boiko, L. S. Paltnik, and A. S. Derevyanchenko, Dokl. Akad. Nauk SSSR **179**, 316 (1968) [Sov. Phys. Dokl. **13**, 237 (1968)].
[5] C. Gao, Y. Wang, A. Ritter, and J. Dennison, Phys. Rev. Lett. **62**, 945 (1989).
[6] J. Tersoff, Phys. Rev. Lett. **61**, 2879 (1988).
[7] G. Galli, R. M. Martin, R. Car, and M. Parinello, Phys. Rev. Lett. **62**, 555 (1989); Phys. Rev. B **42**, 7470 (1990).
[8] D. Beeman, J. Silverman, R. Lynds, and M. R. Anderson, Phys. Rev. B **30**, 870 (1984).
[9] G. Comelli, J. Stöhr, C. J. Robinson, and W. Jark, Phys. Rev. B **38**, 7511 (1988).
[10] D. A. Anderson, Philos. Mag. **35**, 17 (1977).
[11] C. Weissmantel, Thin Solid Films **92**, 55 (1982).
[12] J. C. Angus and C. C. Hayman, Science **241**, 913 (1988).
[13] S. Kaplan, F. Jansen, and M. Machonkin, Appl. Phys. Lett. **47**, 750 (1985).
[14] A. Grill, B. S. Meyerson, V. V. Patel, J. A. Reimer, and M. A. Petrich, J. Appl. Phys. **61**, 2874 (1987).
[15] J. Zelez, J. Vac. Sci. Technol. A **1**, 305 (1983).
[16] J. Cuomo, J. Doyle, J. Bruley, and J. Liu, J. Vac. Sci. Technol. A **9**, 221 (1991).
[17] D. E. Polk, J. Non-Cryst. Solids **5**, 365 (1971).
[18] D. E. Polk and D. S. Boudreaux, Phys. Rev. Lett. **31**, 92 (1973).
[19] N. Savvides, J. Appl. Phys. **58**, 518 (1985); **59**, 4133 (1986).
[20] D. R. McKenzie, D. Muller, and B. A. Pailthorpe, Phys. Rev. Lett. **67**, 733 (1991).
[21] P. H. Gaskell, A. Saeed, P. Chieux, and D. R. McKenzie, Phys. Rev. Lett. **67**, 1286 (1991).
[22] P. C. Kelires, Phys. Rev. Lett. **68**, 1854 (1992).
[23] M. T. Yin and M. L. Cohen, Phys. Rev. B **29**, 6996 (1984).
[24] (a) P. C. Kelires, Europhys. Lett. **14**, 43 (1991); (b) Phys. Rev. B **44**, 5336 (1991).
[25] J. Tersoff, Phys. Rev. B **38**, 9902 (1988).
[26] P. C. Kelires and J. Tersoff, Phys. Rev. Lett. **61**, 562 (1988).
[27] P. C. Kelires and J. Tersoff, Phys. Rev. Lett. **63**, 1164 (1989).
[28] For a review on the phase diagram of carbon, see F. P. Bundy, Physica A **156**, 169 (1989).
[29] G. Galli, R. M. Martin, R. Car, and M. Parinello, Science **250**, 1547 (1990).
[30] N. Wada, P. J. Gaczi, and S. A. Solin, J. Non-Cryst. Solids **35**, 543 (1980).
[31] J. Robertson and E. P. O'Reilly, Phys. Rev. B **35**, 2946 (1987).
[32] H.-P. Kaukonen and R. M. Nieminen, Phys. Rev. Lett. **68**, 620 (1992).
[33] D. Mildner and J. Carpenter, J. Non-Cryst. Solids **47**, 391 (1982).
[34] K. Sinha, J. Menéndez, O. F. Sankey, D. A. Johnson, W. J. Varhue, J. N. Kidder, P. W. Pastel, and W. Lanford, Appl.

Phys. Lett. **60**, 562 (1992).
[35]M. A. Tamor and C. H. Wu, J. Appl. Phys. **67**, 1007 (1990).
[36]J. E. Smith, M. H. Brodsky, B. L. Crowder, and M. I. Nathan, J. Non-Cryst. Solids **8-10**, 179 (1974).
[37]F. D. Murnaghan, Proc. Natl. Acad. Sci. U.S.A. **30**, 244 (1944).
[38]P. J. Martin, S. W. Filipczuk, R. P. Netterfield, J. S. Field, D. F. Whitnall, and D. R. McKenzie, J. Mater. Sci. Lett. **7**, 410 (1988).
[39]J. Robertson, Phys. Rev. Lett. **68**, 220 (1992).